

# Regenerated cellulose/multiwalled carbon nanotube composite films with enhanced mechanical properties prepared in NaOH/urea aqueous solution

Qian Li<sup>1,a</sup> & Qing Li<sup>2</sup><sup>1</sup>College of Chemistry and Chemical Engineering, Wuhan Textile University, Wuhan 430073, China<sup>2</sup>College of Chemistry and Chemical Engineering, Chongqing University of Science and Technology, Chongqing 404100, China*Received 24 October 2014; revised received and accepted 21 May 2015*

Regenerated cellulose (RC)/multiwalled carbon nanotube (MWCNTs) composite films have been successfully prepared in NaOH/urea aqueous solution by coagulation with H<sub>2</sub>SO<sub>4</sub> solution. The structure and properties of the RC/MWCNTs composite films are investigated by Fourier-transform infrared (FTIR) spectra, wide-angle X-ray diffraction (XRD), optical microscope (OM), scanning electron microscopy (SEM), transmission electron microscopy (TEM), thermogravimetric analysis (TGA) and tensile testing. The results reveal that the MWCNTs disperse well in the cellulose matrix when the content of the MWCNTs is less than 1wt%. MWCNTs in the cellulose matrix maintain the original nanocrystalline structure and properties, weaken the hydrogen-bond formed between the cellulose, decrease the crystallinity of the composite films, but do not apparently reduce the thermal stability of the composite films. Compared to regenerated cellulose films, the mechanical properties of the composite films have been improved to some extent. The tensile strength of the composite films is bound to be 108 MPa, when the amount of MWCNTs is just 0.2wt %.

**Keywords:** Composite films, Multiwalled carbon nanotube, Nanocrystalline, Regenerated cellulose

## 1 Introduction

Carbon nanotubes (CNTs) have attracted tremendous attention due to their unique physiochemical properties<sup>1-3</sup>. Experimental studies and theoretical modeling have demonstrated high Young's modulus, stiffness, and flexibility of CNTs<sup>4</sup>. These outstanding properties combined with their low density and high aspect ratios (up to 1000) make CNTs to be used as an excellent reinforcing agents in polymers. It is generally recognized that the high performance of CNTs in composite strongly depends on the ability to homogeneously disperse throughout the matrix, interfacial bonding and the content<sup>5</sup>. Producing well-dispersed CNTs in a composite is difficult due to the intermolecular 'van der Waals interactions' between the CNTs, thus leading to the formation of aggregates. Some efforts such as high-energy sonication of the CNTs over a prolonged period of time and addition of surfactants have been made to obtain uniform dispersion of CNTs in a polymer matrix<sup>6</sup>. The more flexible way is to introduce various functional groups on the surface of CNTs. For instance, by simply refluxing CNTs with nitric acid or mixed acids, some

functional groups, such as carboxylic, carbonyl, and hydroxyl groups, can be introduced on MWCNTs<sup>7</sup>. With these reactive groups on CNTs, many other organic groups can be derived by routine synthesis<sup>8-10</sup>. During the past decade, poly(ethylene oxide)<sup>11</sup>, poly(vinylidene fluoride)<sup>12</sup>, Polyurethane<sup>13</sup> and many other polymers<sup>14-16</sup> have been employed to prepare CNTs/polymer composite, and the improvement in the properties of composite has been noticed<sup>17-19</sup>. However, there are still little studies on CNT/natural polymer composite<sup>20,21</sup>, particularly on CNTs/ cellulose composite.

Cellulose, one of the most plentiful natural biopolymers, is renewable, biodegradable and biocompatible. It is expected to become a new industrial material on account of its high mechanical stability and inexhaustibility. However, cellulose is difficult to process in solution or as a melt because of its large proportion of intra- and inter-molecular hydrogen bonds, and thus only a few composite functional materials based on CNTs/cellulose have been reported<sup>22</sup>. Zhang *et al.*<sup>23</sup> prepared regenerated cellulose (RC)/multiwalled carbon nanotube (MWCNTs) composite fibres with enhanced mechanical properties and thermal stability in ionic liquid 1-allyl-3-methylimidazolium chloride. Lu *et al.*<sup>24</sup> reported the MWCNTs/lyocell composite

<sup>a</sup> Corresponding author.  
E-mail: whclare@163.com

fibres with increasing mechanical and thermal properties, formed by a dry-wet spinning method in N-methylmorpholine-N-oxide (NMMO). However, CNTs/cellulose composite film prepared from an aqueous solution system has not been reported so far.

Recently, NaOH/urea aqueous solution, precooled to  $-12\text{ }^{\circ}\text{C}$ , has been developed to rapidly dissolve cellulose<sup>25</sup>. Moreover, regenerated cellulose films and fibres with good structure and properties have been prepared successfully from the cellulose dope<sup>26</sup>. Encouraged by these findings, in this study the composite films from cellulose and MWCNTs have been produced in NaOH/urea aqueous solution. Structure, morphology and properties of the nanocomposite films are investigated by FTIR, X-ray diffraction (XRD), optical microscope (OM), scanning electron microscopy (SEM), transmission electron microscopy (TEM), thermogravimetric analysis (TGA) and tensile testing.

## 2 Materials and Methods

### 2.1 Materials

Cellulose (cotton linter pulp) was supplied by Hubei Chemical Fiber Group, Ltd., China. Its viscosity-average molecular weight was determined by viscometry in cadoxen ( $9.25 \times 10^4$  g/mol). MWCNTs (content 95 -98 vol%, diameter 60 - 80 nm, and length 1 - 2  $\mu\text{m}$ ) were purchased from Shenzhen Nanometer Gang Co., Ltd., China. Other reagents, (analytical grade), were used without further purification.

### 2.2 Preparation of RC/MWCNTs Nanocomposite Films

A desired amount of MWCNTs was dispersed into 200 g solution with NaOH/urea/water (7:12:81 by weight). The suspension was stirred overnight at room temperature and then ultrasonicated for 1 h. Finally, the suspension was cooled to  $-12.3\text{ }^{\circ}\text{C}$  in a refrigerator. Cellulose (8.25 g) was immediately dispersed into the suspension under vigorous stirring (5 min) to obtain a cellulose/MWCNTs solution. The well-mixed solution was then poured into a glass plate of the thickness 0.5 mm and then immediately immersed in a 5.6 wt %  $\text{H}_2\text{SO}_4$  aqueous solution for 5 min to coagulate. The resulting composite film was washed with running water and dried in the air. The obtained composite films with addition of 0.2, 0.5, 1.0, 2.0 and 4.0% (wt%) MWCNTs were named as CN-02, CN-05, CN-10, CN-20 and CN-40 respectively. The RC film was prepared from pure cellulose in the solution with

NaOH/urea /water (7:12:81 by weight) using the same method.

### 2.3 Characterization

Fourier-transform infrared (FTIR) spectra were recorded on an FTIR spectrometer (model 1600, Perkin-Elmer Co.). The samples were prepared by using the KBr disk method. Wide-angle X-ray diffraction (XRD) measurement was carried out on XRD diffractometer (D8-Advance, Bruker). The XRD patterns with Cu  $K\alpha$  radiation ( $1.5406 \times 10^{-10}$  m) at 40 kV and 30 mA were recorded in the region of  $2\theta$  from  $6^{\circ}$  to  $50^{\circ}$ . Transmission electron microscopy (TEM) images were taken on a JEOL JEM-2010 (HT) electron microscope at an accelerating voltage of 200 kV. The optical microscopy (OM) of the composite films was taken by Olympus B X 60 microscope (USA). Scanning electron microscopy (SEM) was performed on a FESEM (SEM, SIRION TMP, FEI) by using an accelerating voltage of 20 kV.

The tensile strength ( $\sigma_b$ ) and elongation at break ( $\varepsilon_b$ ) of the composite films were measured by universal tensile tester (CMT6503, Shenzhen SANS Test Machine Co, Ltd, China) at a speed of 5 mm/min respectively<sup>27</sup>. Before testing the mechanical properties in dry state, the films were allowed to rest for at least one week at 60-63.5% RH (saturated NaBr solution at room temperature). Conditioning was achieved to ensure the equilibration of the water content in the films with that of the atmosphere (stabilization of the sample weight). The water content of the composite films was about 12-20%. The mechanical properties of the films in wet state were measured immediately after the film soaking in water for 30 min. Each test was repeated at least five times and the average value was reported.

## 3 Results and Discussion

### 3.1 Characterization

Figure 1 shows the FTIR spectra of the RC film and the RC/MWCNTs composite film. The peaks at  $3418\text{ cm}^{-1}$ ,  $1421\text{ cm}^{-1}$  and  $890\text{ cm}^{-1}$  in the spectrum of RC film are the characteristic absorption peaks of cellulose II<sup>28</sup>. Similar to the RC film, the RC/MWCNTs composite films still keep the characteristic absorption of cellulose II, but the broad peak at  $3418\text{ cm}^{-1}$  is shifted to  $3440\text{ cm}^{-1}$  and gradually becomes narrow with the increase in MWCNT content. The bands at around  $3418\text{ cm}^{-1}$  and  $3440\text{ cm}^{-1}$  are attributed to intra- and inter-molecular hydrogen bonding of cellulose, respectively<sup>29</sup>. This

finding suggests that the incorporation of MWCNTs in the matrix partially destroy the hydrogen-bond between the cellulose, leading to the increase in free hydroxyl and the decrease in hydroxyl bonding. In addition, the peak at  $1239\text{ cm}^{-1}$  is ascribed to C-C vibration absorption, which is greatly enhanced due to the presence of MWCNTs.

Figure 2 shows the XRD patterns of MWCNTs, RC and RC/MWCNTs composite films. MWCNTs present the characteristic diffraction peak at  $2\theta = 25.8^\circ$ , indicating that it has a similar crystal structure to highly oriented pyrolytic graphite. The RC film exhibits three characteristic diffraction peaks at  $2\theta = 12.4^\circ$ ,  $20.2^\circ$ , and  $22.2^\circ$ , assigned to  $(1\bar{1}0)$ ,  $(110)$ , and  $(200)$  planes of cellulose II respectively<sup>30</sup>. Compared

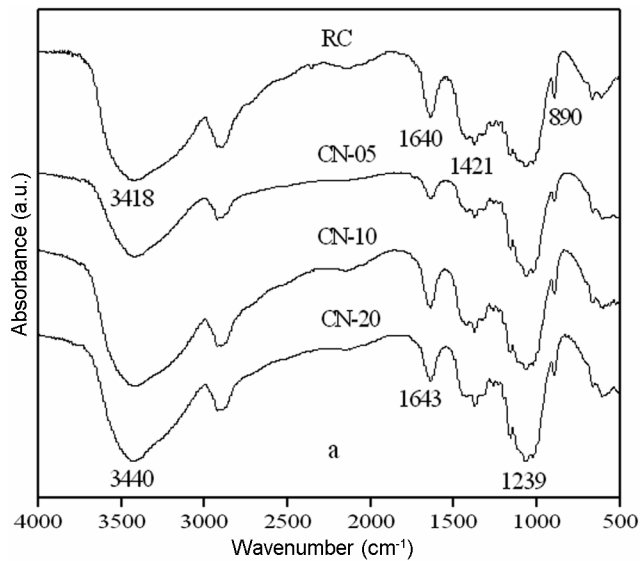


Fig. 1 — FTIR spectra of RC/MWCNT nanocomposite films

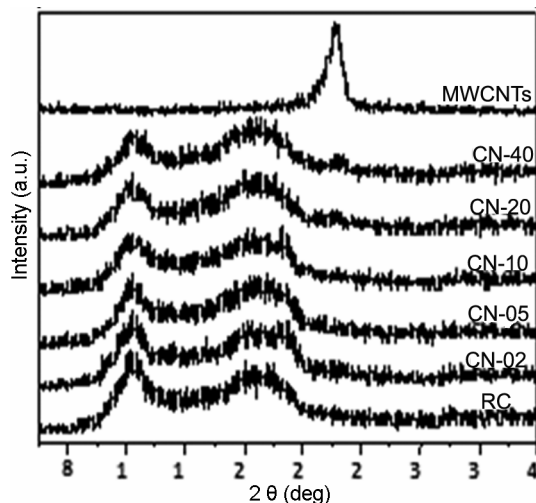


Fig. 2 — XRD patterns of RC/MWCNT nanocomposite films

to the RC film, all the RC/MWCNTs composite films show the typical cellulose II crystalline form, but the shape of the characteristic diffraction peaks of cellulose II becomes broader and the corresponding intensity decreases as the MWCNTs content is increased. These changes imply that the incorporation of MWCNTs has little advancement on the crystalline structure of cellulose. The probable reason could be attributed to the strong interaction between MWCNTs and cellulose chains, which hinders the rearrangement of cellulose chains, leading to the decrease in degree of crystallinity of cellulose. Meanwhile, as the MWCNTs increases in the RC/MWCNTs composite films, a little diffraction peak at  $2\theta = 25.8^\circ$  ascribed to MWCNTs is observed in CN-40 film. The presence of the characteristic diffraction peaks of MWCNTs in the RC/MWCNTs composite films demonstrates that MWCNTs in the cellulose matrix still maintains the original nanocrystalline structure.

### 3.2 Dispersion and Morphology

Figure 3 shows the dispersity of MWCNTs in the cellulose matrix. The carbon nanotubes reflect incident light, and the black dots on the image are the MWCNTs. The optical images of CN-02 and CN-05 composite films show the well-dispersed status of MWCNTs in the matrix with slight aggregation. However, the aggregates of nanotubes are visible in CN-10 and CN-20 composite films. This fact indicates that the MWCNTs are uniformly distributed within the cellulose matrix at lower loading ( $< 1\text{ wt}\%$ ), but there is macrophase separation at higher loading.

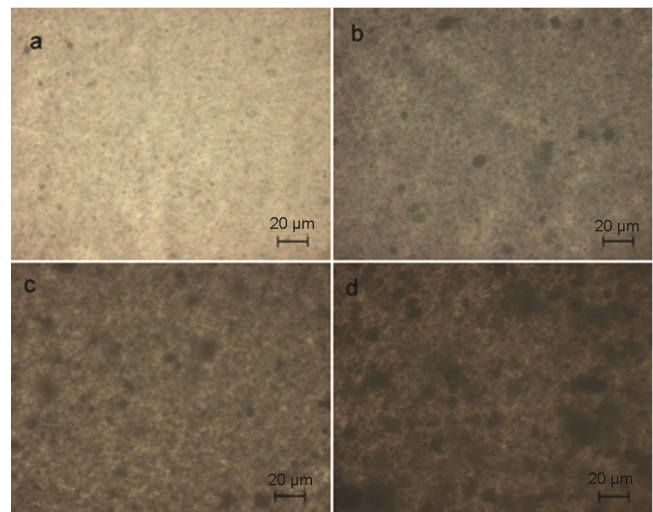


Fig. 3 — Optical microscopic images of RC/MWCNT nanocomposite films (a) CN-02; (b) CN-05; (c) CN-10 and (d) CN-20

TEM was also used to evaluate the dispersion of MWCNTs in cellulose matrix. The variations in contrast and diameter of the MWCNTs are mainly due to difference in electron scattering from different depth regions of the section. As shown in Fig. 4, MWCNTs are dispersed well within the cellulose matrix, and no obvious aggregation is observed even in CN-20 composite film. It is interesting to find that MWCNTs in cellulose matrix presented extreme flexibility and are inter-twined with cellulose. Such entanglement between MWCNTs and cellulose chains, in combination with the nanostructure characteristics of MWCNTs, could provide the structural reinforcement to the cellulose matrix.

Figure 5 shows the fracture surfaces of the RC/MWCNT composite films after tensile testing. The well-dispersed bright dots and lines are the ends of the broken MWCNTs. Due to the traction and stretch orientation in preparation process, the carbon nanotubes in the fractured sample appear to be aligned along one direction. From Figs 5(a) and (b), a homogeneous dispersion of MWCNTs is achieved throughout the cellulose matrix at 0.5 wt % MWCNTs loading, and the fraction surface of CN-05 composite film show clear and large layer shape structure. With 4.0 wt % MWCNTs loading [Figs 5 (c) and (d)],

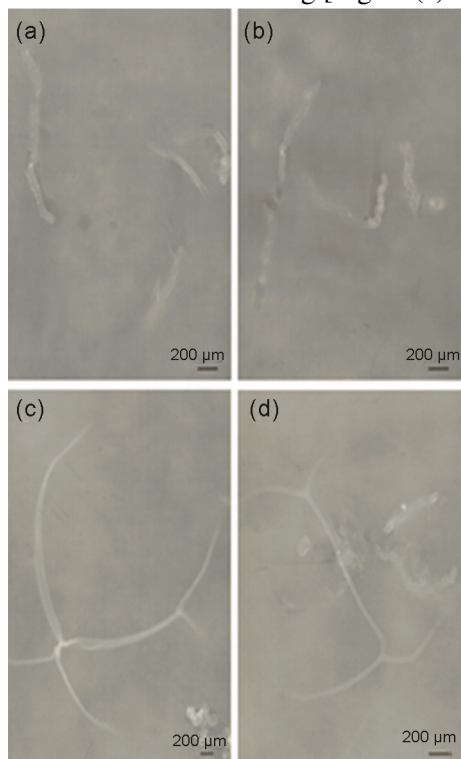


Fig. 4 — TEM images of the RC/MWCNT nanocomposite films. (a) CN-02; (b) CN-05; (c) CN-10 and (d) CN-20

the fraction surface of CN-40 composite film becomes small and part of the MWCNTs tends to aggregate. These results further prove that MWCNTs is compatible with cellulose matrix at lower loading but separated from cellulose matrix at higher loading.

### 3.3 Thermal Stability

Thermal degradation patterns of the RC and the RC/MWCNTs composite films are shown in Fig. 6. The RC/MWCNTs composite films have a similar thermal decomposition behavior to the RC film, and all of them present three obvious steps of thermogravimetry. In the first step, a small weight loss of about 3.0-6.0 wt % at 50-150 °C could be assigned to the release of moisture from the samples. In the second step, the greatest weight loss, attributed to the decomposition of cellulose, is found in the temperature range 250-350 °C for the RC and the RC/MWCNTs composite films. In the third step, the

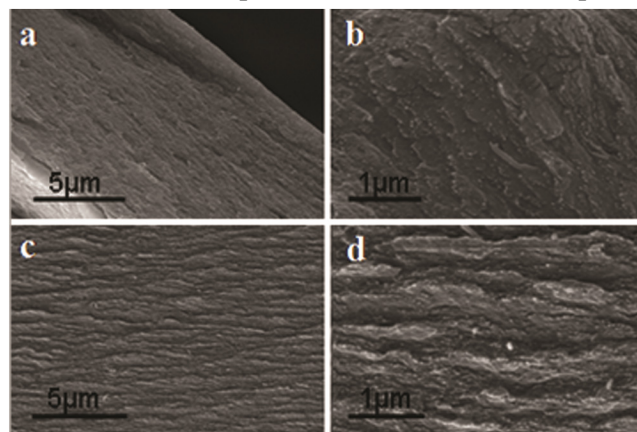


Fig. 5 — SEM images of fracture surface of the RC/MWCNT nanocomposite films, (a and b) CN-05 and (c and d) CN-40

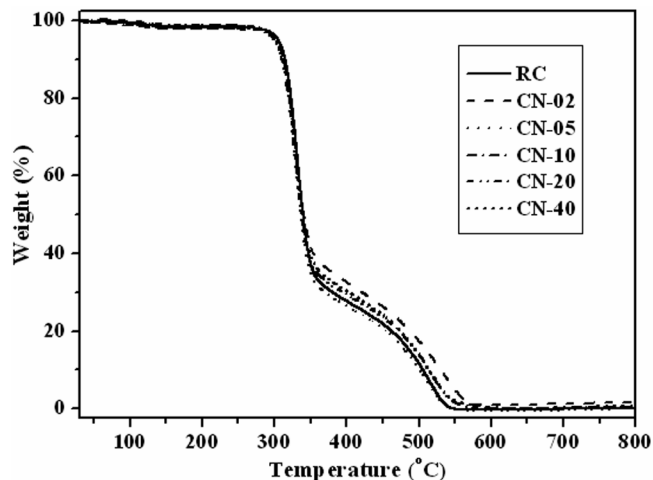


Fig. 6 — TGA curves of the RC/MWCNT nanocomposite films



weight loss at 350-550 °C is believed to be caused by oxidation and carbonization of the samples. At this step, it is interesting to observe that the RC/MWCNTs composite films show quicker oxidation and carbonization rate in comparison with that of the RC films. This phenomenon could be explained by the high thermal conductivity of the MWCNTs, which accelerates the process of the oxidation and carbonization in RC/MWCNTs composite films. The TGA results indicate that the introduction of MWCNTs in cellulose matrix does not apparently reduce the thermal stability of the matrix, and suggests some extent of miscibility between cellulose and nanotubes.

### 3.4 Tensile Test

The elongation-at-break ( $\epsilon_b$ ) and tensile strength ( $\sigma_b$ ) are plotted as a function of MWCNTs content (Fig. 7). There is a significant relationship between mechanical properties of composite films and the MWCNTs content. The incorporation of MWCNTs greatly improves the tensile properties of the composite films especially with lower MWCNTs content. With addition of 0.2 wt % MWCNTs,  $\sigma_b$  and  $\epsilon_b$  increase by about 16.7% and 69.3% in contrast with neat RC film. As MWCNTs loading is increased to 1.0 wt %,  $\sigma_b$  and  $\epsilon_b$  are further enhanced by 31.9% and 165% respectively. However, the improvement in these properties declines when more MWCNTs are incorporated (2.0-4.0 wt %). With 2.0 wt% of MWCNTs filler,  $\epsilon_b$  is increased slightly, while  $\sigma_b$  is almost kept stable. As the loading level of MWCNTs is increased to 4.0 wt%, both  $\sigma_b$  and  $\epsilon_b$  dramatically reduce. In view of the above results, it is concluded that the reinforcement effect on mechanical properties

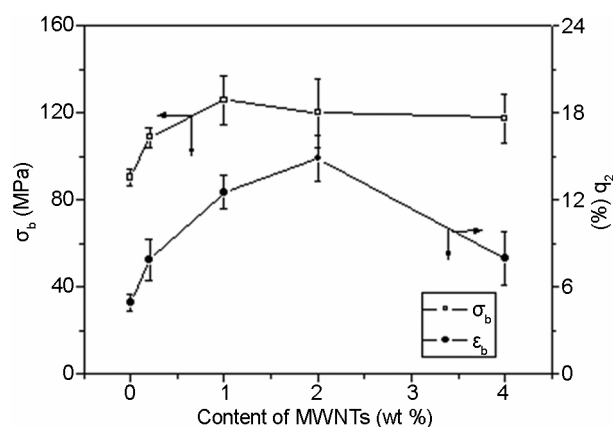


Fig. 7 — Tensile strength ( $\sigma_b$ ) and elongation at break ( $\epsilon_b$ ) of the RC/MWCNT nanocomposite films

and tensile properties could be ascribed to the finely dispersed high performance MWCNTs nanofillers throughout the cellulose matrix. MWCNTs in cellulose matrix present extreme flexibility, while the carbon nanotubes appear to be aligned along one direction for the traction and stretch orientation in preparation process. On the other hand, the aggregate of MWCNTs within the matrix at higher concentrations increases the film defect, thus partially offsetting the reinforcement effect.

### 4 Conclusion

Regenerated cellulose (RC)/multiwalled carbon nanotube (MWCNTs) composite films are successfully prepared via a simple and green method. The formed composite films are characterized by FTIR, XRD, OM, SEM, TEM, TGA and tensile testing. The MWCNTs are observed to be homogeneously dispersed throughout the cellulose matrix at lower loading (< 1 wt %), but separated from cellulose matrix at higher loading. For the entanglement between MWCNTs and cellulose chains, the incorporation of MWCNTs leads to decrease in the degree of crystallinity of cellulose, but does not apparently reduce the thermal stability of the matrix. As expected, tensile test shows that both the mechanical properties and the tensile properties of the RC/MWCNTs composite films are greatly improved at lower MWCNTs loading for the effect of nano enhancement. However, these reinforcement effects are declined due to the aggregate of MWCNTs within the matrix at higher concentrations.

### References

- Baughman R H , Zakhidov A A & de Heer W A, *Science*, 297 (2002) 787.
- Thostenson E T, Ren Z F & Chou T W, *Compos Sci Technol*, 61 (2001) 1899.
- Bhagat N A, Shrivastava N K, Suin S, Maiti S & Khatua B B, *Polym Compos*, 34 (2013) 787.
- Xie X , Mai Y W & Zhou X P, *Mater Sci Eng*, 49 (2005) 89.
- Gong X, Liu J, Baskaran S, Voise R D & Young J S, *Chem Mater*, 12 (2000) 1049.
- Zhi Y, Chen X, Pu Y, Zhou L, Chen C, Li W, Xu L, Yi B & Wang Y, *Polym Adv Technol*, 18 (2007) 458.
- Pirlot C, Willems I, Fonseca A, Nagy J B & Delhalle J, *Adv Eng Mater*, 4 (2002) 109.
- Barghamadi M & Behmadi H, *Polym Compos*, 33 (2012) 1085.
- Li Y Y, Wang B & Li X L, *Polym Compos*, 32 (2011) 1352.
- Neelgund G M, Oki A & Luo Z, *Colloid Surface B*, 100 (2012) 215.
- Ratna I D, Jagtap I S B, Rathor R, Kushwaha R K, Shimpi N & Mishra S N, *Polym Compos*, 34 (2013) 1003.
- Yao S H, Yuan J K, Zhou T & Dang Z M, *J Phys Chem C*, 115 (2011) 20011.
- Athanasopoulos N, Baltopoulos A, Matzakou M, Vavouliotis A & Kostopoulos V, *Polym Compos*, 33 (2012) 1302.

- 14 Zhao X & Ye L, *J Polym Sci B*, 48 (2010) 905.
- 15 Naffakh M, Díez-Pascual A M, Marco C & Ellis G, J, *Mater Chem*, 22 (2012) 1418.
- 16 Kumar B, Kumar I & Singh R P, *Polym Compos*, 30 (2009) 855.
- 17 Chakraborty G, Gupta K, Rana D & Meikap A K, *Polym Compos*, 33 (2012) 343.
- 18 Biercuk M J, Llaguno M C, Radosavljevic M, Hyun J K, Johnson A T & Fischer J E, *Appl Phys Lett*, 80 (2002) 2767.
- 19 Lin J, Zhang L, Chen W & Li C Z, *Polym Compos*, 34 (2013) 1313.
- 20 Pan H, Zhang Y, Hang Y, Shao H, Hu X & Xu Y, *Biomacromolecules*, 13 (2012) 2859.
- 21 Gomathi P, Kim M K, Park J J & Ragupathy D, *Sensor Actuat B*, 155 (2011) 897.
- 22 Wu X, Zhao F, Varcoe J R, Thumser A E, Avignone-Rossa C & Slade R C, *Bioelectrochem*, 77 (2009) 64.
- 23 Zhang H, Wang Z G, Zhang Z N, Wu J, Zhang J & He J S, *Adv Mater*, 19 (2007) 698.
- 24 Lu J, Zhang H H, Jian Y H, Shao H L & Hu H C, J, *Appl Polym Sci*, 123 (2012) 956.
- 25 Cai J & Zhang L, *Macromol Biosci*, 5 (2005) 539.
- 26 Mao Y, Zhou J P, Cai J & Zhang L, *J Membr Sci*, 279 (2006) 246.
- 27 Liu J, Yue Z & Fong H, *Small*, 5(2009)536
- 28 Bora U, Sharma P & Kannan K, *J Biotechnol*, 126 (2006) 220.
- 29 Kondo T, Sawatari C, Manley R S J & Gray D G, *Macromolecules*, 27 (1994) 2130.
- 30 Zhang L, Mao Y, Zhou J P & Cai J, *Ind Eng Chem Res*, 44 (2005) 522.